Optimal reflection-free complex absorbing potentials for quantum propagation of wave packets

Oded Shemer, Daria Brisker, and Nimrod Moiseyev*

Department of Chemistry and Minerva Center of Nonlinear Physics in Complex Systems, Technion – Israel Institute of Technology, Haifa 32000, Israel

(Received 3 June 2004; revised manuscript received 15 November 2004; published 23 March 2005)

The conditions for optimal reflection-free complex-absorbing potentials (CAPs) are discussed. It is shown that the CAPs as derived from the smooth-exterior-scaling transformation of the Hamiltonian [J. Phys. B **31**, 1431 (1998)] serve as optimal reflection-free CAPs (RF CAPs) in wave-packet propagation calculations of open systems. The initial wave packet, $\Phi(t=0)$, can be located in the interaction region (as in half collision experiments) where the CAPs have vanished or in the asymptote where $\hat{V}_{CAP} \neq 0$. *As we show, the optimal CAPs can be introduced also in the region where the physical potential has not vanished*. The unavoided reflections due to the use of a finite number of grid points (or basis functions) are discussed. A simple way to reduce the "edge-grid" reflection effect is described.

DOI: 10.1103/PhysRevA.71.032716 PACS number(s): 03.65.Nk, 02.70.−c, 31.15.−p

I. INTRODUCTION

There is an extensive use in wave-packet (WP) propagation calculations in complex absorbing potentials (CAPs). The use of CAPs in propagation of WP calculations is usually for half collision experiments where the initial wave packet is localized in the interaction region where the CAPs have vanished. The role of the CAPs is to avoid the reflection from the edge of the grid as obtained in the numerical propagation calculations. Often CAPs are referred to as optical potentials. The CAPs are used in very different fields of physics, chemistry, and technology. See, for example, calculations of resonances for CAPs in a nuclear physics problem [1]; deriving different expressions that simplify the numerical calculations of state-to-state transitions probabilities for reactive scattering collisions (for time-independent Hamiltonians see Ref. [2] and for time-dependent ones see Ref. [3]); calculations of complex molecular potential-energy surfaces by CAPs [4]; and molecular electronic studies where the CAP serves to absorb charge reaching the electrodes [5]. Besides the use of CAPs in the numerical calculations an effort has been taken in developing different types of CAPs. See, for example, Refs. [6–12] where recently different types of CAPs were developed. For a most recent review on CAPs see Ref. [13].

In 1998 we have derived CAPs by applying the smooth-exterior-scaling transformations (SESs) to the Hamiltonian [14]. Here we study the *conjecture* that the use of exterior-scaling or SES similarity transformations produce reflection-free CAPs (RF CAPs) for the WP propagation calculations. As we will show here within the finite basis-set or finite grid approximations the CAPs are not reflection-free ones. However, it is possible to show that for a given finite basis/grid method a quantity criteria for the strength of the numerical reflections can be derived. It is important to mention that about the same time Riss and Mayer [15] obtained CAPs, which under specific conditions are similar to the SES CAPs, by taking another approach (so-called transformative CAP). Only when the CAP is introduced in a region where the potential energy has vanished, the transformative CAP derived by Riss and Meyer [15] is equal to the SES CAP that has been derived analytically without any approximations by us [14] (in such a case the SES CAP and the transformative CAP are identical although they look slightly different). Our main motivation for deriving SES CAPs was to simplify the calculations of resonances positions and widths. However, this SES CAP has been used also to avoid the artificial reflections from the edge of the grid in wave-packet (WP) propagation calculations [16]. One may wonder, what is the need for the transformative CAPs or the SES CAPs since the reflections can be taken as small as one wishes by introducing the CAP in the domain where the physical potential is zero and by making the CAP (any CAP) soft and long enough [17]. The answer to that question is that it is most desired to avoid the use of long-ranged CAPs which require a large number of basis functions or a large number of grid points in heavy duty numerical calculations. For example, in propagation calculations of many electron molecular systems it is hard to avoid the introduction of the CAP in the domain where the physical long-range potential is not zero.

Here we want to discuss two types of questions. The first type is mathematical-physical questions (i.e., theoretical questions in the sense that we assume that complete basis sets are used), such as the following:

(i) What are the properties of reflection-free CAPs? (As we show here, there are two conditions that should be satisfied.)

(ii) Can we introduce the RF CAP in the domain where the physical potential is not zero and the propagated wave packet does not consist of outgoing waves only? (As we show, the answer is yes.)

(iii) Can the initial state be exponentially localized in the interaction region, as required in half collision experiments, where the CAP vanishes? (The answer is yes.)

(iv) Can the initial state be localized in the domain where $V_{CAP} \neq 0$? (The answer is yes, provided the smooth-exterior

*Author to whom correspondence should be addressed: Electronic address: nimrod@tx.technion.ac.il

scaling transformation is applied to the initial state.)

The second type is practical questions.

(i) Are indeed the RF CAPs reflection free in the numerical calculations where a finite number of grid points or a finite number of basis functions are used? (The answer is no since in spite of the complete absorbing of the fast moving components of the wave packet still there is an edge-grid reflection effect which is associated with the slow moving components of the WP.)

(ii) Can we minimize the reflections which result from the use of finite-sized basis/grid methods and how? (The answer is yes, by methods explained in the paper.)

(iii) Can we apply the RF CAPs to many-electron problems? (The answer is yes provided the electronic repulsion terms, $1/|\vec{r}_i-\vec{r}_j|$, are modified. This requirement can be avoided when the ionized electrons are not correlated.)

II. WHAT ARE THE IDEAL REFLECTION-FREE CAPS ?

First, we should describe the numerical problem we want to solve by introducing a CAP into the Hamiltonian. Using the Hermitian quantum mechanics the propagated wave packet is given by

$$\Phi_{exact}(t) = e^{-i\hat{H}t/\hbar}\Phi_{0.} \tag{1}$$

In the numerical calculations the propagated wave packet is $\Phi_{num}(t) \neq \Phi_{exact}(t)$. We are looking for numerical methods for which

$$|\Phi_{num}(t) - \Phi_{exact}(t)| < \epsilon, \tag{2}$$

where ϵ determines the requirement accuracy from the numerical results. Since in the numerical calculations only a finite number of grid points or a finite number of basis functions are used, the available spatial space is not from $r=0$ to $r=\infty$ but up to $r=L$. Therefore accurate results are obtained as long as $\Phi_{exact}(t)$ vanishes at $r \geqslant L$. By increasing the number of the grid points or by increasing the number of the basis functions we increase the value of L. The initial state Φ_0 is a square integrable function. In half collision experiments (such in photodissociative or autoionization reactions) the initial WP is localized in the interaction region where $|\Phi_{num}(t=0)-\Phi_{exact}(t=0)| < \epsilon$. However, as time passes the wave packet spreads and only during a given period of time τ, the numerical calculations satisfy the accuracy condition stated above. It is important to realize that the value of τ is determined by the time it takes for the tail of the wave packet to reach the edge of spatial space (i.e., $r=L$). In order to obtain $\Phi_{num}(t)$ within the desired accuracy, one should increase the number of the used grid/basis points/functions and thereby increase the value of L. *The role of the CAP is to enable one to obtain accurate numerical results in the limited available spatial space, $r \leqslant r_{CAP} < L$, without the need to increase the number of grid/basis points/functions*. Namely,

$$\Phi_{CAP}(t) = e^{-i(\hat{H}+\hat{V}_{CAP})t/\hbar}\Phi_0, \tag{3}$$

where due to the use of the finite grid/ basis-set numerical methods,

$$\Phi_{CAP}(r \geqslant L, t) = 0. \tag{4}$$

The CAP is defined such that

$$\hat{V}_{CAP} = 0 \; as \; r \leqslant r_{CAP} < L \tag{5}$$

and

$$|\Phi_{CAP}(t) - \Phi_{exact}(t)| < \epsilon \text{ in the region where } \hat{V}_{CAP} = 0. \tag{6}$$

A common requirement is that

$$\Phi_0 = 0 \text{ in the region where } \hat{V}_{CAP} \neq 0. \tag{7}$$

As a matter of fact, the last condition is too strong and it is possible to satisfy Eq. (6) also when the initial state is localized in the region where the CAP gets nonzero values. This extension will be discussed later.

Short-range CAPs (the Saxson-Wood potential) have been used about two decades ago in molecular wave-packet calculations [18]. A CAP which has been used often in the literature [19–34] is $V_0=0$ for $x<x_0$ and $V_0=-i\lambda(x-x_0)^n$ where $n=1, 2, \ldots 8$ for $x \geqslant 0$. For large values of n these CAPs are very similar to the purely imaginary step-type potential that has been shown above to provide a strong reflection. Regarding the reflections due to the introducing of abrupt complex potentials one might be aware of the fact that there are examples (see the review in Ref. [13], and references therein) of discontinuous potentials that are constructed to avoid reflection, and absorb totally, at single incident energies, or in certain momentum intervals, or at a discrete set of energies. Of course they cause reflections at other energies. The CAPs that we are looking for are different ones. They are energy-independent RF CAPs, and in principle can be chosen to be universal ones (i.e., problem independent).

As we will show here it is unlikely to have a universal (i.e., problem independent) CAP for which both Eqs. (4) and (6) are satisfied. Therefore let us first discuss the possibility to satisfy Eq. (6) when the condition given by Eq. (4) is replaced by a weaker numerical condition: $\Phi_{CAP}(t)$ is a square integrable function at any given time, which decays to zero much *faster* than the exact solution. Such that within a given time interval

$$\Phi_{CAP}(r = L(T), t < T) \leqslant \epsilon, \tag{8}$$

where the value of ϵ is determined from the desired accuracy of the numerical calculations.

III. SES TRANSFORMATIONS AND THE CONDITIONS FOR OPTIMAL REFLECTION-FREE CAPS

The idea of introducing RF CAPs by using the exterior scaling or SES methods is clear: the Hamiltonian remains as it is inside the inner region, where the coordinates stay on the real axis. However, it has been shown by Simon that upon the exterior scaling transformation,

$$r \rightarrow r_{ext}, \tag{9}$$

where inside the inner unscaled region,

$$r_{ext} = r \text{ when } r \leqslant r_{CAP}, \tag{10}$$

and in the external-scaled region,

$$r_{ext} = r_{CAP} + (r - r_{CAP})e^{i\theta} \text{ when } r > r_{CAP}, \tag{11}$$

the eigenfunctions are *not equal* to eigenfunctions of the unscaled (i.e., Hermitian) problem *inside* the unscaled region [35]. For example, for a free particle Hamiltonian the continuum eigenfunctions inside the inner unscaled region are given by $A_{in}\exp[-ik\exp(-i\theta)r]+A_{out}\exp[+ik\exp(-i\theta)r]$. Since the propagated WP can be described as a linear combination of the eigenfunctions of the complex scaled (or exterior scaled) Hamiltonian, it is not clear at all that in this case Eq. (6) is satisfied (here we consider the exterior scaled Hamiltonian as $\hat{H}+\hat{V}_{CAP}$). This result is very confusing since from numerical propagation calculations we know that inside the inner unscaled region in space, the propagated WP is exactly as obtained without the use of exterior scaling. As we will show below the validity Eq. (6) can be easily explained by association the SES approach with the use of similarity transformation operators as developed in Refs. [14,36]. Using the SES approach,

$$r \rightarrow r_{SES} \equiv F_\theta(r), \tag{12}$$

where the path in the complex coordinate space is chosen such that

$$|F_\theta(r) - r| \leqslant \epsilon \text{ when } r < r_{CAP} \tag{13}$$

and

$$\frac{F_\theta(r)}{r} \rightarrow e^{i\theta} \quad \text{as} \quad r \rightarrow \infty. \tag{14}$$

The SES transformations clearly show that Eq. (6) can be satisfied to any desired accuracy. If the SES transformation is represented by the similarity operator $\hat{S}$, then the propagated WP within the framework of the SES approach is given by $\hat{S}\Psi_{exact}(t)$ which is equal to $\Psi_{exact}(t)$ inside the inner region [see Eq. (13)] where $\hat{S}\sim 1$.

Let us discuss now the validity of Eq. (8). Following Simon's proof for the exterior scaled potential and following Moiseyev and Hirschfelder's proof for general complex scaled transformations [37] (including the SES transformations), the complex scaled resonances functions are square integrable but the continuum eigenfunctions are not square integrable functions. They are associated with complex eigenvalues, $E_{ext}(\text{continuum}) = k_{ext}^2/2 = [k\exp(-i\theta)]^2/2$, such that $k_{ext}\, r_{ext}$ in the *exterior* region is equal to the same value as obtained in Hermitian quantum mechanics, i.e., $k\, r$ (note that a very different result is obtained in the inner region as discussed in the previous paragraph). Therefore the asymptote of the continuum wave functions as obtained after the application of the exterior or SES transformations remain as obtained within the framework of the conventional (i.e., Hermitian) quantum-mechanical (QM) approach. Upon complex scaling k_{ext} is rotated into the lower-half complex k plane to avoid the exponential divergence of the complex scaled incoming waves associated with real and positive values for the wave vector, i.e.,

$$\exp(-ikr_{ext}) = \exp[-ik\cos(\theta)r]\exp[+k\sin(\theta)r] \rightarrow \infty,$$

as $r\rightarrow\infty$. Therefore it is not obvious whether a square integrable WP such as $\Phi_{exact}(t)=\int_{-\infty}^{+\infty}C(k,t)\exp(ikr)dk\rightarrow 0$ as $r\rightarrow\infty$ remains square integrable when $r\rightarrow r_{ext}$ or $r\rightarrow r_{SES}$. It has been proven by Moiseyev and Katriel [38] that for sufficiently small values of θ, i.e., $\theta<\theta_c$, the eigenfunctions of a complex scaled Hamiltonian which are associated with the bound states are square integrable. The value of θ_c depends on the shape of the potential [38]. Let us assume that the wave packet is a Gaussian, $\exp(-ar^2)$. It is clear that $\exp(-ar_{ext,SES}^2)$ remains square integrable provided that $\theta \leqslant \theta_c = \pi/2$. When the wave packet is more localized, for example is described as $\exp(-ar^N)$, then $\theta_c = \pi/N$. Since Gaussians form an overcomplete basis set, one might expect that any square integrable function (which can be expanded in term of the Gaussian basis set) remains square integrable after applying the complex scaling or the SES transformation.

It is easy to prove that the wave packet $\Phi_{exact}(t)$ decays exponentially to zero at any given time, provided it is a square integrable function at $t=0$. A proof which holds also for complex scaled non-Hermitian Hamiltonians is as follows: $\Phi_{exact}(t+dt)=\exp(-i\hat{H}dt/\hbar)\Phi_{exact}(t)$. For sufficiently small values of dt, $\exp(-i\hat{H}dt/\hbar)=\Sigma_{n=0}(n!)^{-1}(-idt/\hbar)^n(\hat{H})^n$ is a converged series (provided $\text{Im}\hat{H}\leqslant 0$). If $\Phi_{exact}(t'\leqslant t)$ is a square integrable function then $(\hat{H})^n\Phi_{exact}(t)$ is square integrable as well [the second derivative of a square integrable function is square integrable and the product of a square integrable function and a confined (complex scaled) potential is also a square integrable function].

Let us summarize the facts we know by now: (i) when the initial wave-packet (WP) is square integrable the time propagated WP is square integrable as well; (ii) the complex scaled square integrable WP remains square integrable; (iii) the complex scaled incoming waves diverge exponentially whereas the outgoing waves exponentially decay to zero; (iv) in the absence of a source of particles in infinite large distance from the studied system, the asymptote of the propagated WP consists of outgoing waves only (as in half collision experiments). From (i)–(iii) it is clear that for the most general case the square integrable WP,

$$\Phi_{exact}(r \geqslant L,t) = \int_0^\infty dk[D(k,t)e^{-ikr} + C(k,t)e^{+ikr}] \rightarrow 0 \text{ as } r\rightarrow\infty, \tag{15}$$

remains square integrable,

$$\Phi_{CAP}(r \geqslant L,t) = \int_0^\infty dk[D(k,t)e^{-ik\cos(\theta)r}e^{+k\sin(\theta)r} + C(k,t)e^{+ik\cos(\theta)r}e^{-k\sin(\theta)r}] \tag{16}$$

$$\rightarrow 0 \text{ as } r\rightarrow\infty, \tag{17}$$

although each one of the components of the complex scaled incoming waves exponentially diverge. When the condition (4) is not satisfied, this fact (i.e., interference of exponen-

tially diverged incoming waves results in a square integrable function) may introduce some numerical difficulties in the propagation calculations. For overcoming these types of numerical difficulties when long-ranged potentials are used see the second reference in Ref. [29].

When condition (iv) is satisfied (as in all half collision experiments) then

$$\Phi_{exact}(r \geqslant L,t) = \int_0^\infty dk C(k,t) e^{+ikr} \rightarrow 0 \text{ as } r \rightarrow \infty, \tag{18}$$

and it is easy to see that Φ_{CAP} decays faster since

$$\Phi_{CAP}(r \geqslant L,t) = \int_0^\infty dk C(k,t) e^{+ik\cos(\theta)r} e^{-k\sin(\theta)r}. \tag{19}$$

The fact that within the interval of $r_{CAP} < r \leqslant L$, the propagated WP, $\Phi_{CAP}(t)$, decays *faster* than $\Phi_{exact}(t)$ is the main motivation behind the use of the exterior scaling, smooth-exterior complex scaling methods in the numerical propagation calculations.

IV. A QUANTITY CRITERIA FOR THE MEASUREMENT OF THE STRENGTH OF THE NUMERICAL REFLECTIONS

From Eq. (19) a quantity criteria for the strength of the numerical reflections from the edge of the grid is obtained,

$$|C(k,t)e^{-k\sin(\theta)L}| \leqslant \epsilon. \tag{20}$$

As an upper limit for the accuracy of the calculations one gets that

$$|C(k,t)e^{-kL}| \leqslant \epsilon. \tag{21}$$

At $t=0$ the initial wave packet gets exponentially small values at $r \geqslant L$ and therefore we can consider it as a case where $C(k,0)=0$. As time passes the wavelet with the largest value of k (associated with a large velocity) is the first to reach the edge of the grid. As one can see from Eq. (21) the fast moving components of the wave packet are entirely absorbed at $r=L$, due to the use of the complex absorbing boundary conditions which were introduced by the use of the exterior scaling or the SES transformations. For the components of the wave packet associated with small values of k, the requirement of $\exp(-kL) \sim 0$ is satisfied by increasing the value of L. The propagation calculations using SES transformations, within the framework of the finite basis-set/grid approximations, are accurate as long as $|C(k,t)|$ gets sufficiently small values. This explains why L in Eq. (8) is a function of time and why the duration of the propagation calculations cannot exceed a given period of time T when L is held fixed in the propagation calculations.

As an illustrative example we carried out wave-packet propagation calculations for a one-dimensional Gaussian, $\Psi(x,t=0)=(1/5\pi)^{1/4}\exp(-x^2/10+ip_0x)$, which is localized at a potential well embedded in between two identical potential barriers. This potential, $V(x)=(0.5x^2-0.8)\exp(-0.1x^2)$, has been used before as a test problem for methods developed in non-Hermitian quantum mechanics (see, for example, Ref. [36] and references therein). In Fig. 1 the results obtained from two types of propagation calculations are presented. The long dashed line stands for the numerically exact calculations of $\Psi_{exact}(x,t=60)$, using a fifth-order split operator with $-1000 \leqslant x \leqslant +1000$. The full solid line is $\Psi(F_{\theta=0.5\ rad}(x),t=60)$ where $F_\theta(x)$ is a smooth exterior scaling function, such that $F_\theta \sim x$ when $|x| < x_{CAP} \equiv 90$, whereas $F_\theta = x\exp(i\theta)$ when $|x| > x_{CAP}$. For $|x| < x_{CAP}$ $\Psi_{exact}(x,t=60) \approx \Psi(F_\theta(x),t=60)$. However, it is clearly shown that unlike the exact wave packet which oscillates, the smooth exterior scaled wave packet [labeled in Fig. 1 by non-Hermitian quantum-mechanics (NH-QM) approach] decays to zero as x is rotated into the complex coordinate plane around $x=x_{CAP}=90$.

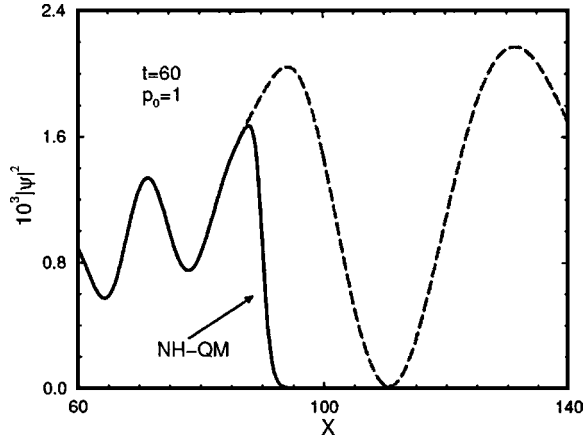

FIG. 1. The numerical exact propagated wave packet (long dashed line), $\Psi_{exact}(x,t=60)$, and the corresponding wave packet (denoted by NH-QM) which is defined as $\Psi(F_{\theta=0.5\ \mathrm{rad}}(x),t=60)$. The smooth-exterior-scaling contour is defined as $F_\theta \sim x$ when $|x| < x_{CAP} \equiv 90$, whereas $F_\theta = x\exp(i\theta)$ when $|x| > x_{CAP}$. The initial wave packet is given by $\Psi(x,t=0)=(1/5\pi)^{1/4}\exp(-x^2/10+ip_0x)$, where $p_0=1$.

Following our analysis the propagated wave packet decays to zero when the contour x is smooth exterior scaled (rotated) into the complex coordinate space only within the time interval $t \leqslant T$. The results presented (denoted by NH-QM) in Fig. 2 were obtained from numerical calculations where $-100 \leqslant x \leqslant +100$ (i.e., the box size is $L=200$). It is clearly shown that until $t \leqslant 30$ the complex scaled wave packet is practically equal to zero at the edge of the grid (i.e., at $x=L/2$). As time exceeds the value of $t=T \equiv 30$ the complex scaled wave packet is reflected from the edge of the grid.

V. HOW TO REDUCE THE NUMERICAL REFLECTIONS OF THE SLOW MOVING COMPONENTS OF THE WAVE PACKET FROM THE EDGE OF THE GRID

Let us propose two different possibilities:

(a) *Accelerate the slow moving components of the wave packet by inducing an external dc field.* Equation (21) indicates clearly that the numerical reflections from the edge of the grid are associated with slow moving wavelengths. As

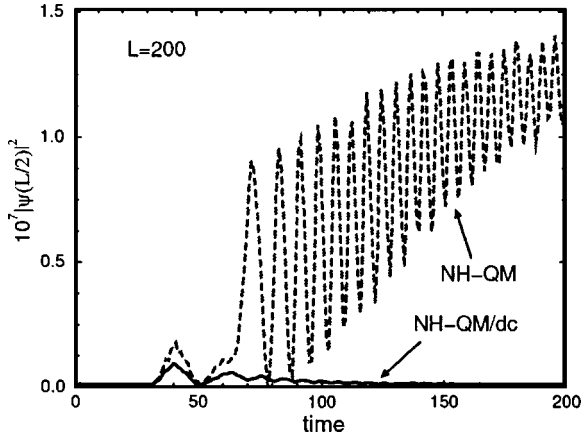

FIG. 2. The non-Hermitian propagated wave packet which is constructed from 400 Fourier basis functions (long dashed line, denoted by NH-QM) as a function of time at $x=L/2$ (edge of the grid). The propagated wave packet is defined as $\Psi(F_{\theta=0.5\ \mathrm{rad}}(x=100),t)$, such that $F_\theta \sim x$ when $|x|<x_{CAP}\equiv 90$, whereas $F_\theta = x\exp(i\theta)$ when $|x|>x_{CAP}$. The initial wave packet is given by $\Psi(x,t=0)=(1/5\pi)^{1/4}\exp(-x^2/10+ip_0x)$, where $p_0=0$. The reflections from the edge of the grid as time passes are obtained when $t>T\equiv 30$. The full line stands for the results obtained when a dc field has been introduced close to the edge of the grid, $x_{dc}=95$ and $\mathcal{E}_{dc}=2$.

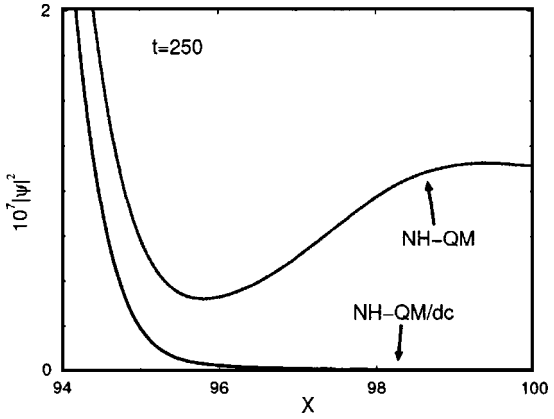

FIG. 3. The numerical propagated wave packets at $t=250$ as obtained when 400 Fourier functions were used as a basis set. The reflections from the edge of the grid (which appear at $t>30$ as shown in Fig. 2) are avoided as a dc field is added close to the edge of the grid.

discussed above, the fast moving components of the wave packet are entirely absorbed at $r=L$, due the use of the SES CAPs. A possible solution to this problem is by adding a static field close to the edge of the grid, in order to accelerate the slow moving wavelengths which are completely absorbed by the SES CAPs. The static field is turned on only at the edge of the grid where $r\geqslant r_{dc}$ and is given by

$$V_{ext-dc}(r\geqslant r_{dc}) = -\frac{\mathcal{E}_{dc}}{2}(r-r_{dc}). \tag{22}$$

The value of r_{dc} and $\mathcal{E}_{dc}$ can be optimized to minimize the effect of the dc field on the WP propagation. An estimate of the error introduced by adding the V_{ext-dc} potential term to the Hamiltonian can be obtained from the imaginary parts of the bound states calculated for the Hamiltonian which is taken as $\hat{H}+V_{ext-dc}+\hat{V}_{CAP}$. The evaluation of $\hat{V}_{CAP}$ from the SES transformations will be described in Sec. VI.

Let us return to our illustrative numerical example. The smooth exterior scaled wave packet has been calculated as described above when $|x|\leqslant 100$ (i.e., the box size is $L=200$) when V_{ext-dc} dc-potential term was added into the Hamiltonian. The results presented in Fig. 2 (the full solid line denoted by NH-QM/dc) clearly show the strong suppression of the reflections from the edge of the grid as the dc field has been introduced into the Hamiltonian. In Fig. 3 we present the numerical results obtained at $t=250$. It is clearly shown that close to the edge of the grid the dc field inhibits the artificial reflections as appeared in the NH-QM calculations. Note that as time passes the reflection leads to the distortion of the wave packet also at regions which are quite far from the edge of the grid, as shown in Fig. 4. However, as one can see from the results presented in Fig. 4 the introducing of the static field reduces this artificial edge-grid reflection effect.

(b) *Imposing of outgoing boundary conditions.* The numerical edge-grid reflection effect can be reduced by imposing outgoing boundary conditions (complex scaled ones in our case). It is simple to implement that approach when grid methods are used,

$$\vec{\Phi}_{CAP}(t+\Delta t) = \mathrm{U}\vec{\Phi}_{CAP}(t), \tag{23}$$

where $\mathbf{U}(t+\Delta t \leftarrow t)$ is the time evolution $N\times N$ matrix and the jth component of the vector $\vec{\Phi}_{CAP}(t)$ is the value of the propagated WP at $\vec{r}_j$; $j=1,2,\ldots N$ grid point. The grids points are ordered such that $|\vec{r}_1|\leqslant|\vec{r}_2|\leqslant\cdots|\vec{r}_{N-1}|\leqslant|\vec{r}_N|$. The notation of CAP stands for the use of the exterior or the SES transformations. The outgoing boundary conditions are im-

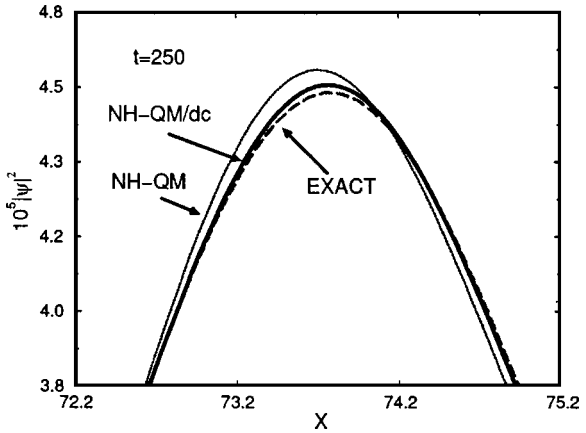

FIG. 4. The propagated wave packets at $t=250$ as obtained when 400 Fourier functions were used as a basis set, in a comparison with the numerically exact solution. The propagated wave packet as obtained when both the smooth exterior scaling transformation and the dc field were implemented into the numerical calculations is in a very good agreement with the numerical exact solution.

posed by replacing the Nth row of the time evolution matrix $U_{N,i};\ i=1,2,\ldots,N$ by $\exp[i\exp(i\theta)\vec{k}(\vec{r}_N-\vec{r}_{N-1})]U_{N-1,i}$. Here we use the fact that the $\vec{r}_N$, $\vec{r}_{N-1}$, $\vec{r}_{N-2}$ grid points are in the scaled region where $\vec{r}\rightarrow\vec{r}\exp(i\theta)$. The wave vector $\vec{k}$ is determined from the previous time step calculations and from the $\vec{r}_{N-1}$ and the $\vec{r}_{N-2}$ grid points. That is,

$$\exp[i\exp(i\theta)\vec{k}(\vec{r}_{N-1}-\vec{r}_{N-2})]=\frac{\Phi_{CAP}(\vec{r}_{N-1},t)}{\Phi_{CAP}(\vec{r}_{N-2},t)}. \quad (24)$$

It should be stressed that it is not always true that at a given time the tail of the WP is constructed of a single outgoing wave component. However, this kind of an approximation has been found useful in WP propagation calculations of various physical problems [39].

One should assure that the real part of the wave vector gets positive values only. In the one-dimensional case where equally spaced grid points are used, the application of that approach is straightforward. In such a case the modified last row of the time evolution matrix is given by

$$U_{N,i}(t+\Delta t\leftarrow t)=U_{N-1,i}(t+\Delta t\leftarrow t)\frac{\Phi_{CAP}(r_{N-1},t)}{\Phi_{CAP}(r_{N-2},t)}. \quad (25)$$

Similarly, one can modify all $j>j_c$ rows and not only the last one. The assumption is that the vectors $\vec{r}_{j>j_c}$ are all embedded in the asymptote region of the propagated wave packet. This method (applicable to three-dimensional problems as well) to reduce the edge-grid reflection effect is an extension/variation of Hadley's original work, where the transparent boundary condition for the beam propagation method was developed [39]. This method does not require the use of CAPs. However, we believe that the use of the exterior or the SES transformation together with the transparent boundary condition should minimize the numerical reflections from the edge of the grid.

The possibility to impose the outgoing boundary condition by modifying the time evolution operator as shown in Eq. (25) is illustrated here by applying it to our test-case problem. The results presented in Fig. 5 clearly show that by using the method introduced above a similar absorbing boundary condition effect—as achieved when the RF CAPS are added to the Hamiltonian—is obtained. A comparison between the results presented in Figs. 5 and 1 shows that the RF CAP (Fig. 1) provides better results than those obtained by imposing the outgoing boundary condition on the propagated wave packet (Fig. 5). However, it might be expected that similarly to the effect of the dc field described above, the combination of the two approaches would avoid the reflections which are obtained after long time propagation. This study is out of the scope of the present study and requires further investigation.

VI. OPTIMAL RF CAPS FROM THE SES TRANSFORMATIONS

In order to complete the representation of optimal RF CAPs we should show that under well defined specific conditions the use of the SES transformation is equivalent to the

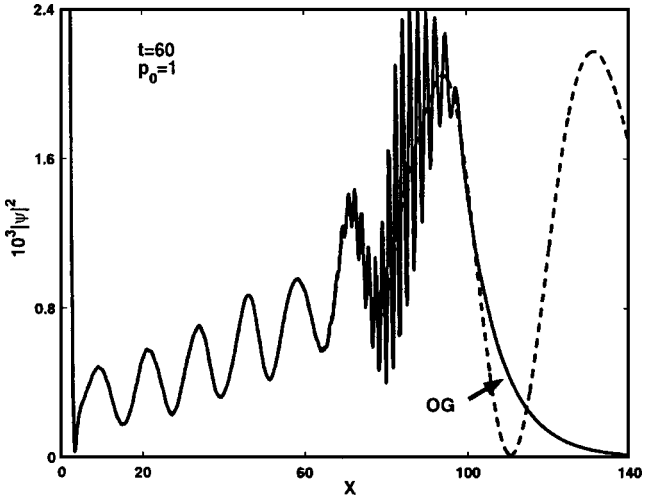

FIG. 5. The propagated wave packet as obtained when the time evolution operator has been modified as explained in the text [see Eq. (25)]. The model Hamiltonian and the initial state are as described in the caption of Fig. 1. The long dashed line stands for the results obtained from numerically exact propagation calculations.

inclusion of a CAP which gets nonzero values only in the edge of the grid. This SES CAP is a nonlocal operator, since it includes terms with the momentum and kinetic energy operators. For the sake of a coherent representation of the subject we briefly describe how the SES CAPs are obtained.

The SES transformed time-dependent Schrödinger equation can be rewritten as

$$\mathcal{H}_{CAP}\Phi_{CAP}(t)=i\frac{\partial}{\partial t}\Phi_{CAP}(t), \quad (26)$$

where

$$\mathcal{H}_{CAP}=\hat{S}\hat{H}\hat{S}^{-1}, \quad (27)$$

$$\Phi_{CAP}=\hat{S}\Phi_{exact}(t)=\Phi_{exact}(F_\theta(r),t). \quad (28)$$

We have proved before that the SES transformation is equivalent to the including of a nonlocal energy-independent, universal (i.e., problem independent) CAP [14],

$$\mathcal{H}_{CAP}=\hat{H}+\Delta V+\hat{V}_{RF\text{-}CAP}, \quad (29)$$

where the correction term to the physical potential is given by

$$\Delta V=V(F_\theta(r))-V(r), \quad (30)$$

and the nonlocal energy-independent, universal CAP has been proved to be equal to [14]

$$\hat{V}_{RF\text{-}CAP}=V_0(r,\theta)+V_1(r,\theta)\frac{\partial}{\partial r}+V_2(r,\theta)\frac{\partial^2}{\partial r^2}. \quad (31)$$

The complex functions $V_j;\ j=0,1,2$ have vanished in the inner region where $r<r_{CAP}$. They are inverse proportional to the mass (reduced mass) of the particle(s) which is (are) absorbed by the $\hat{V}_{RF\text{-}CAP}$ and are defined as [note that below we use the notation $F_\theta^{(n)}(r)\equiv dF_\theta^n(r)/dr^n$] [14]

$$V_0(r,\theta)=\frac{\hbar^2}{4M(F_\theta^{(1)}(r))^3}\left[F_\theta^{(3)}(r)-\frac{5(F_\theta^{(2)}(r))^2}{2F_\theta^{(1)}(r)}\right], \quad (32)$$

$$V_1(r,\theta)=\frac{\hbar^2 F_\theta^{(2)}(r)}{M(F_\theta^{(1)}(r))^3}, \quad (33)$$

$$V_2(r,\theta)=\frac{\hbar^2}{2M}[1-(F_\theta^{(1)}(r))^{-2}]. \quad (34)$$

The initial state is defined as

$$\Phi_0(\text{transformed})=\Phi(F_\theta(r),t=0). \quad (35)$$

When the initial state is localized in the interaction region where $\hat{V}_{RF\text{-}CAP}=0$ then $\Phi(F_\theta(r),t=0)=\Phi(r,t=0)$. In the case that the physical potential is a short-range potential it is quite obvious that the contour of integration $F_\theta(r)$ can be chosen to yield $\Delta V=0$ everywhere at any point in the entire space. In the case of long-range potential the situation is more complicated [40]. In such a case the ΔV term in Eq. (29) cannot be neglected and the SES RF CAP is equal to $\Delta V+\hat{V}_{RF\text{-}CAP}$ and seems to be problem dependent. However, for neutral molecules if r_{CAP} gets a sufficient large value such that the ionized electrons are in hydrogeniclike orbitals then $\Delta V+\hat{V}_{CAP}$ can be replaced by a universal potential term $1/r-1/F_\theta(r)+\hat{V}_{RF\text{-}CAP}$ [40]. This approach holds also for many-electron systems where we assume that the ionized electrons are not correlated as they get far away from the atom/molecule/QD. In such a case we do not need to replace the two electron repulsion terms $|\vec{r}_i-\vec{r}_j|^{-1}$ by $|F_\theta(\vec{r}_i)-F_\theta(\vec{r}_j)|^{-1}$.

Before concluding let us return to our illustrative numerical example. Using 400 Fourier basis functions (with the box size, $L=200$) we obtained matrix representations of the Hermitian Hamiltonian, $\hat{H}_{H\text{-}QM}=-0.5d^2/dx^2+(0.5x^2-0.8)\exp(-0.1x^2)$, and also of the non-Hermitian one, $\hat{H}_{NH\text{-}QM}=\hat{H}_{H\text{-}QM}+\hat{V}_{RF\text{-}CAP}$. The parameters for the function $F_\theta(x)$ as defined in Refs. [14,16] are $\theta=0.5$ rad, $\lambda=0.9$ and $x_{CAP}=90$. The two 400×400 matrices were diagonalized. The eigenvalues and eigenvectors of the Hermitian matrix are correspondingly given by $E_j^{H\text{-}QM}$(real) and $\vec{C}_j^{H\text{-}QM}$. Similarly, $E_j^{NH\text{-}QM}$(complex) and $\vec{C}_j^{NH\text{-}QM}$ are associated with the eigenvalues and eigenvectors of the non-Hermitian (complex and symmetric) matrix. The propagated wave packet within the framework of H-QM is given by

$$\Psi_{H\text{-}QM}(x,t)=\sum_{j=1}^{400}e^{-iE_j^{H\text{-}QM}t}\sum_n C_{n,j}^{H\text{-}QM}\exp\left(i\frac{2\pi nx}{L}\right). \quad (36)$$

The propagated wave packet within the framework of the NH-QM approach is given by

$$\Psi_{NH\text{-}QM}(x,t)=\sum_{j=1}^{400}e^{-iE_j^{NH\text{-}QM}t}\sum_n C_{n,j}^{NH\text{-}QM}\exp\left(i\frac{2\pi nx}{L}\right). \quad (37)$$

The results presented in Fig. 6 clearly show that while the reflections from the edges of the grid appeared in the propagation calculations within the framework of the conventional QM, they do not show up in the NH-QM calculations. The reflections appeared in the conventional quantum-mechanical calculations due to the use of the eigenfunctions, which were obtained within the framework of the box-quantization approximation, as a basis set. A quasidiscrete continuum rather than a continuous continuum has been used in the propagation calculations. As one can see from the results presented in Fig. 6 the use of the RF CAP provides $\Psi_{NH\text{-}QM}(-90<x<+90,t=60)=\Psi_{exact}(-90<x<+90,t=60)$ (within more than six digits of accuracy). In spite of the fact that in the two calculations we have used the same basis functions and the same number of them the NH-QM calculations provided an accurate propagated wave packet while the conventional calculations are far from convergence.

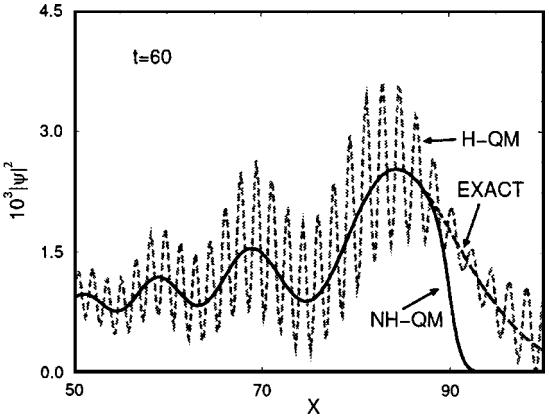

FIG. 6. The propagated wave packets at $t=60$ as obtained from conventional and non-Hermitian QM calculations, in a comparison with the numerically exact solution (denoted by a long dashed line). The propagated wave packets denoted by H-QM and NH-QM correspondingly were constructed from the eigenfunctions and eigenvalues of the Hermitian and non-Hermitian Hamiltonians when 400 Fourier basis functions were used as a basis set. The NH-QM results obtained when the smooth-exterior-scaling transformation was introduced (by adding $\hat{V}_{RF\text{-}CAP}$ into the Hermitian Hamiltonian), are in a complete agreement with the exact solution when $|x|<x_{CAP}\equiv90$.

VII. CONCLUDING REMARKS

We can summarize it by saying that for the CAPs derived from the SES transformations [14]: (i) the propagated WP decays faster to zero than the exact solution and therefore at any given time we can use a smaller grid/basis in the numerical calculations when the SES CAPs are introduced into the numerical calculations; (ii) the SES CAPs can be introduced also in the region where the interaction potential is active (provided the edge of the grid is in the region where the exact WP has outgoing wave components only); (iii) the use of SES CAPs enables one to introduce the CAPs also in the region where the initial WP does not get zero values; (iv) the duration of the WP calculations which provide accurate results (avoiding the numerical reflections from the edge of the grid) can be easily estimated (see Fig. 3); (v) it is possible to reduce the reflections of the slow moving components of the wave packet, either by introducing a dc field in the edge of

the grid or by imposing outgoing boundary conditions on the propagated WP. (vi) The SES CAPs are indeed the optimal reflection-free caps, RF CAPS, for wave-packet propagation calculations.

ACKNOWLEDGMENTS

This work was supported in part by the Israel Science Foundation (Grant No. 73/01) and by the Fund of Promotion of Research at the Technion. One of us (N.M.) acknowledges Juan G. Muga (the correspondence author of a recent review on CAPs) from Bilbao for drawing his attention to the open question: what are the perfect reflection-free CAPs for the motion of wave-packet calculations? It is a pleasure to thank Hans-Dieter Meyer from Heidelberg for his most helpful comments and Yoav Berlatzky from the Technion for drawing our attention to Ref. [39].

[1] H. Masui and Y. K. Ho, Phys. Rev. C **65**, 054305 (2002).
[2] W. H. Thompson and W. H. Miller, Chem. Phys. Lett. **206**, 123 (1993).
[3] I. Vorobeichik and N. Moiseyev, J. Phys. B **31**, 645 (1998).
[4] R. Santra and L. S. Cederbaum, J. Chem. Phys. **117**, 5511 (2002).
[5] R. Baer, T. Seidman, S. Ilani, and D. Neuhauser, J. Chem. Phys. **120**, 3387 (2004).
[6] B. Poirier and T. Carrington, Jr., J. Chem. Phys. **118**, 17 (2003).
[7] S. Feuerbacher, T. Sommerfeld, R. Santra, and L. S. Cederbaum, J. Chem. Phys. **118**, 6188 (2003).
[8] D. E. Manolopoulos, J. Chem. Phys. **117**, 9552 (2002).
[9] A. Neumair and V. A. Mandelshtam, Phys. Rev. Lett. **86**, 5031 (2001).
[10] R. Santra and T. Sommerfeld, Int. J. Quantum Chem. **82**, 218 (2001).
[11] F. Gemperle, F. X. Gadea, and Ph. Durand, Chem. Phys. Lett. **291**, 517 (1998).
[12] U. V. Riss and H.-D. Meyer, J. Chem. Phys. **105**, 1409 (1996).
[13] J. G. Muga, J. P. Palao, B. Navarro, and I. L. Equsquiza, Phys. Rep. **395**, 357 (2004).
[14] N. Moiseyev, J. Phys. B **31**, 1431 (1998).
[15] U. V. Riss and H.-D. Meyer, J. Phys. B **31**, 2279 (1998).
[16] R. Zavin, I. Vorobeichik, and N. Moiseyev, Chem. Phys. Lett. **288**, 413 (1998).
[17] H.-D. Meyer (private communication).
[18] C. Leforestier and R. E. Wyatt, J. Chem. Phys. **78**, 2334 (1983); **82**, 752 (1985).
[19] G. Jolicard and E. J. Austin, Chem. Phys. Lett. **121**, 106 (1985).
[20] G. Jolicard and E. J. Austin, Chem. Phys. **103**, 295 (1986).
[21] G. Jolicard and M. Y. Perrin, Chem. Phys. **116**, 1 (1987).
[22] G. Jolicard, C. Leforestier, and E. J. Austin, J. Chem. Phys. **88**, 1026 (1988).
[23] D. Neuhauser and M. Baer, J. Chem. Phys. **92**, 3419 (1990).
[24] M. Baer, C. Y. Ng, and D. Neuhauser, Chem. Phys. Lett. **169**, 534 (1990).
[25] D. Neuhauser, M. Baer, and D. J. Kouri, J. Chem. Phys. **93**, 2499 (1990).
[26] D. Neuhauser, R. S. Judson, M. Baer, and D. J. Kouri, Comput. Phys. Commun. **63**, 460 (1991).
[27] I. Last, D. Neuhauser, and M. Baer, J. Chem. Phys. **96**, 2017 (1992).
[28] G. Jolicard and G. D. Billing, J. Chem. Phys. **97**, 997 (1992).
[29] U. Peskin and N. Moiseyev, J. Chem. Phys. **96**, 2347 (1992); **97**, 2804 (1992).
[30] V. A. Mandelshtam and H. S. Taylor, J. Chem. Phys. **103**, 2903 (1995).
[31] T. P. Grozdanov, V. A. Mandelshtam, and H. S. Taylor, J. Chem. Phys. **103**, 7990 (1995).
[32] D. Neuhauser, J. Chem. Phys. **103**, 8513 (1995).
[33] U. V. Riss and H.-D. Meyer, J. Chem. Phys. **105**, 1409 (1996); A. Jackle and H.-D. Meyer, *ibid.* **105**, 6778 (1996).
[34] R. Santra and L. S. Cederbaum, Phys. Rep. **368**, 1 (2002).
[35] B. Simon, Phys. Lett. **71A**, 211 (1979).
[36] N. Moiseyev, Phys. Rep. **302**, 211 (1998).
[37] N. Moiseyev and J. O. Hirschfelder, J. Chem. Phys. **88**, 1063 (1988).
[38] N. Moiseyev and J. Katriel, Chem. Phys. Lett. **105**, 194 (1984).
[39] G. R. Hadley, IEEE J. Quantum Electron. **28**, 363 (1992).
[40] S. Klaiman, I. Gilary, and N. Moiseyev, Phys. Rev. A **70**, 012709 (2004).